Hindawi Publishing Corporation
International Journal of Photoenergy
Volume 2013, Article ID 791438, 8 pages
http://dx.doi.org/10.1155/2013/791438

Research Article

Corrosion Monitoring of Flexible Metallic Substrates for Dye-Sensitized Solar Cells

Trystan Watson, Gavin Reynolds, David Wragg, Geraint Williams, and David Worsley

SPECIFIC, College of Engineering, Swansea University, Baglan Bay Innovation Centre, SA12 7AX Port Talbot, UK

Correspondence should be addressed to Trystan Watson; t.m.watson@swansea.ac.uk

Received 24 May 2013; Accepted 10 July 2013

Academic Editor: Shahed Khan

Copyright © 2013 Trystan Watson et al. This is an open access article distributed under the Creative Commons Attribution License, which permits unrestricted use, distribution, and reproduction in any medium, provided the original work is properly cited.

Two techniques for monitoring corrosion within a dye-sensitized solar cell (DSC) system are presented, which enable continuous, high sensitivity, in situ measurement of electrolyte breakdown associated with DSCs fabricated on metals. The first method uses UV/Vis reflectance spectrophotometry in conjunction with encapsulation cells, which incorporate a 25 μm thick electrolyte layer, to provide highly resolved triiodide absorption data. The second method uses digital image capture to extract colour intensity data. Whilst the two methods provide very similar kinetic data on corrosion, the photographic method has the advantage that it can be used to image multiple samples in large arrays for rapid screening and is also relatively low cost. This work shows that the triiodide electrolyte attacks most metals that might be used for structural applications. Even a corrosion resistant metal, such as aluminium, can be induced to corrode through surface abrasion. This result should be set in the context with the finding reported here that certain nitrogen containing heterocyclics used in the electrolyte to enhance performance also act as corrosion inhibitors with significant stabilization for metals such as iron. These new techniques will be important tools to help develop corrosion resistant metal surfaces and corrosion inhibiting electrolytes for use in industrial scale devices.

1. Introduction

Nanostructured dye-sensitized solar cells (DSCs) are a third generation solar cell, where production costs have the potential to be considerably lower than that of rival silicon PV devices [1]. The materials used are easily available, no specialised environments are needed for production, and the technology may also be incorporated onto flexible materials such as strip metal products [2–7]. There is significant interest related to the fabrication of DSC technology onto cladding and roofing material as building integrated photovoltaics [8].

The DSC is a photoelectrochemical device consisting of a dye-coated semiconductor photoelectrode and a counter electrode arranged in a sandwich configuration, with the interelectrode space filled with a liquid electrolyte, usually containing an iodine/triiodide (I_3^-/I^-) redox mediator. When dye molecules are excited by visible light, they inject electrons into the conduction band of a TiO_2 semiconductor support on which they are anchored. The role of the redox mediator in the electrolyte is to reduce the oxidised dye molecule back to the ground state, allowing a continuous production of electrons under illumination. The oxidized form of the redox mediator is reduced at the counter electrode according to (1) by electrons transported via an external electrical connection:

$$I_3^- + 2e^- \longrightarrow 3I^- \quad (1)$$

Although traditional devices employ conductive glass electrodes, the use of cheaper metal substrates to transport electrons from the semiconductor is desirable in large scale DSC devices since it will allow for continuous roll-to-roll processing. The electrolyte used in DSC is known to corrode some industrial sheet metals such as zinc-coated carbon steel [2]. Titanium and stainless steel are possible flexible substrates for DSC [4, 5, 9–11] as they have been shown to be resistant to corrosion by the nonaqueous I_3^-/I^- electrolyte [2]. The iodide present in the electrolyte is capable of depassivating an oxide covered metal surface (in an analogous manner to chloride ions) the reducing triiodide providing a facile cathodic reaction to couple with anodic metal dissolution. Recent work has confirmed that

in addition to titanium, stainless steel and inconel (nickel-chromium alloy) do not seem to corrode in the presence of the redox mediator used as photoelectrodes within a cell setup [12–14]. This confirms previous findings [4, 6] where both aluminium and copper electrodes were also found to corrode in systems with flexible polymer top sheets. However, despite the reported work described previously, no convenient quantitative method of studying the time-dependent interaction of metallic substrates with DSC electrolyte within a convenient timescale currently exists. The work reported here seeks to address this by describing two new rapid methods of characterising the reaction kinetics of tri-iodide with a wide range of potential metal substrates for DSC applications.

The reduction of the tri-iodide into iodide ions is characterised by a change in the electrolyte colour, yellow/brown to transparent, which in turn decreases the number of charge carrying species and leads to inferior device performance. The aim of this current study is to develop techniques which could allow in situ measurement of the corrosion rates of metals in sealed cells, without the need for ex situ sampling of the DSC electrolyte. We have adapted two techniques used in other areas of DSC study, such as dye uptake kinetics, namely, diffuse reflectance UV-visible spectrophotometry (DR-UV/Vis) and time-lapse digital photography [15–18]. As both techniques employ thin electrolyte layers in contact with metal surfaces, any interaction of the coloured tri-iodide species with the metal can be rapidly quantified. Time-resolved UV/Vis spectrophotometry has been employed in order to monitor colour change within the thin electrolyte layer, enabling even subtle changes to be detected over considerable timescales. The time-lapse photography method, coupled with analysis of red, green, and blue (RGB) intensity values, enables a far greater number of cells to be studied in a single experiment.

2. Materials and Methods

2.1. Materials. The metal substrates studied in this work, along with their purity and compositions, are shown in Table 1. All of them were purchased from Goodfellow Metals Ltd.

2.2. Preparation of Model DSC Corrosion Cells. Metal substrate coupons of dimensions 50 mm × 50 mm × 2 mm were firstly abrasively polished using 1200 grit silicon carbide paper (unless specified otherwise as in the case of aluminium), washed in water and mild detergent, and then rinsed with ethanol. The glass top layer used for the corrosion cell construction had dimensions of 50 mm × 50 mm and was also washed in water and mild detergent, followed by rinsing with ethanol. In order to replicate the environment in which DSC electrolyte and a metal substrate interact within a DSC, encapsulation corrosion cells were produced, where a 25 mm × 25 mm × 25 μm volume of electrolyte was introduced to the metal through bonding the sections of glass to the substrate using a 25 μm thick Surlyn (DuPont Ltd.) gasket that had been laser-cut to the required specifications. Holes of 0.5 mm diameter were conveniently drilled through the glass for the introduction of the redox electrolyte into the cell.

Table 1: Metals used and their purity.

Metals	Purity
Nickel	99.98% Ni
Aluminium	99.999% Al 99.9% Al
Inconel 625	61% Ni, 22% Cr, 9% Mo, 5% Fe
Iron	99.5% Fe
Titanium	99.6% Ti
Molybdenum	99.9% Mo
Stainless steel 316	18% Cr, 10% Ni, 3% Mo
Stainless steel 304	18% Ni, 10% Cr
Zinc	99.9% Zn
Tungsten	99.95% W
Chromium	99.95% Cr

The electrolyte can vary significantly in its makeup related to inclusion of additives. The most basic redox couple consists of only lithium iodide and iodine dissolved in 3-methoxypropionitrile or acetonitrile. 4-tert-butylpyridine (TBP) or N-methylbenzimidazole are also widely added to the electrolyte and said to significantly improve open circuit voltage (V_{oc}) and cell efficiency due to their ability in reducing back reaction effects by blocking the triiodide molecule from interacting with the titania surface [19]. Additions of guanidinium thiocyanate are used to enhance ion transport efficiency [20], and iodine-based ionic liquids such as 1-propyl-3-methylimidazolium iodide (PMII) are added to reduce viscosity and in turn enhance ion mobility within the electrolyte. In this experiment, a very simple DSC electrolyte solution was selected initially in order to isolate the effect of the iodide/tri-iodide redox couple without the interaction of the other electrolyte additives such as TBP or guanidinium thiocyanate. For this reason, unless otherwise stated, 0.1 M LiI and 0.05 I_2 dissolved in 3-methoxypropionitrile was prepared and introduced to each cell, respectively, by vacuum injection and the remaining hole sealed with Surlyn and a circular microscope coverslip. Subsequent experiments demonstrate the influence of TBP on substrate corrosion.

2.3. Time-Lapse DR-UV/Vis Spectrophotometric Analysis. Metal photoelectrode corrosion activity was studied using a Perkin Elmer Lambda 750 S UV/Vis spectrophotometer with a 60 mm integrating sphere to monitor the absorbance change of the I_3^- redox mediator over time, when placed in contact with each metal substrate. The spectrophotometer was used in reflectance mode, and the encapsulation cells were placed against the reflectance opening of the integrating sphere so that only the electrolyte region was in the beam path and angled with respect to the beam so that the reflected light was carried to the detector as shown by the schematic representation in Figure 1.

The monochromatic light beam was able to pass through the glass top layer and the 25 μm thick electrolyte medium

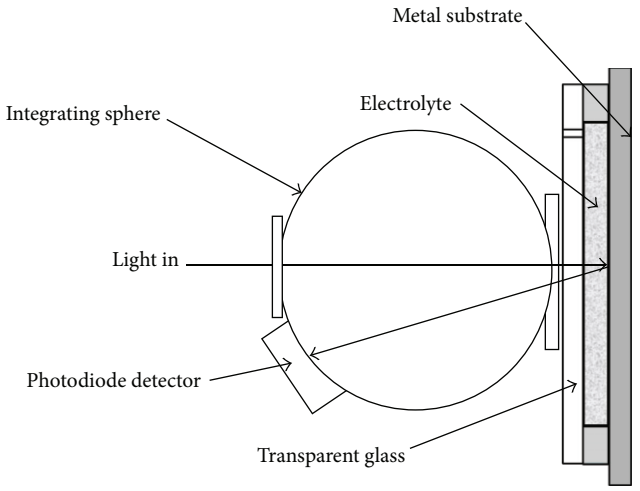

Figure 1: Schematic representation of UV/Vis setup when used in reflectance.

and can be reflected at the polished metal substrate. Experiments were carried out in situ using a time-lapse setup, where absorption spectra over a wavelength range between 300 nm and 800 nm were recorded at 5 minute intervals for 24 hours. The absorption spectra were analysed at the tri-iodide absorption wavelength (~410 nm) to find the rate of I_3^- disappearance. Preliminary experiments were carried out in situ for the first 24 hours to capture any sudden disappearance of I_3^-. Metals which had not corroded in this time period were subjected to further ex-situ tests for longer time periods thereafter.

Both the change in RGB values and absorption spectra relating to I_3^- disappearance for the various metals were then compared in order to draw up a ranking of corrosion resistance.

2.4. Digital Time-Lapse Image Acquisition. Digital image capture was trialled as a method of recording corrosion rates since it is far more convenient and cheaper than DR-UV/Vis. The aim was to evaluate whether the data obtained was consistent between the techniques. Digital images were collected in a dark room environment using a Canon Powershot G10 digital camera at 5 minute intervals for 100 hours from approximately 20 cm above the corrosion cells immediately after introducing electrolytes into each cell; the setup is shown schematically in Figure 2. Consistent light was provided by a UV-filtered tungsten halogen lamp. Subsequent image analysis was carried out using a software package (Sigma Scan Pro), and the data was recorded in RGB format with colour intensity graded from 0 to 256 (dark to light), so numbers increased as corrosion proceeded. Average RGB values from selected regions of the electrolyte interaction area were then plotted against time, correlating to the rate of I_3^- disappearance. The samples were then photographed periodically beyond this time at longer intervals up to 1000 hours for signs of corrosion.

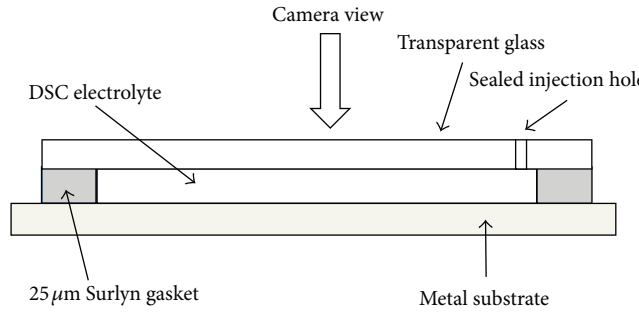

Figure 2: Configuration of corrosion encapsulation test cell and camera view.

3. Results and Discussion

The degradation phenomenon being studied here is the redox process occurring at the metal substrate/electrolyte interface. The metal is oxidised by the tri-iodide according to (2):

$$\mathrm{M} + \left(\frac{x}{2}\right)\mathrm{I_3}^- \longrightarrow \mathrm{M}^{x+} + \left(\frac{3x}{2}\right)\mathrm{I}^-, \quad (2)$$

where M is the metal substrate and x refers to its oxidation state. The loss of colour observed is due to the triiodide being reduced to iodide ions. The two techniques presented here provide complimentary knowledge on the corrosion timescales of metals in contact with a typical dye-sensitized solar cell electrolyte layer. A range of different metals has been tested to demonstrate the techniques with an initial focus on iron and titanium representing differing performance in electrolyte exposure tests.

Firstly, considering the DR-UV/Vis method, the time-dependant changes in absorption spectra for both iron and titanium following addition of the electrolyte are shown for illustration in Figures 3(a) and 3(b).

By using the decrease in the I_3^- absorption maxima, a plot of absorbance over time can be generated as shown in Figure 4. This enables identification of the point of corrosion onset and completion (i.e., when no further colour change is observed). Performing single sample UV-Vis analysis over 100 hours timeframe is not a viable tool for industrial analysis; therefore, an analogous tool was developed using time-lapse photographic imaging. The rate of change of the I_3^- is demonstrated for iron and titanium for both techniques in Figure 4.

There is a clear correlation between the observed change in the DR-UV/Vis absorption values and the average RGB value. This suggests that both techniques can be used for corrosion analysis with the photographic method having the advantages of cost and the ability for simultaneous sample analysis.

The corrosion of iron, shown in Figure 4, is significant since it is perhaps the most important structural metal that DSC could be applied to in large areas for roofing and walling. Previously published work has suggested that carbon steel surfaces show little evidence of degradation in the presence of the DSC electrolyte [2]. Here, as shown in Figures 3 and 4, this has been observed to occur within 2

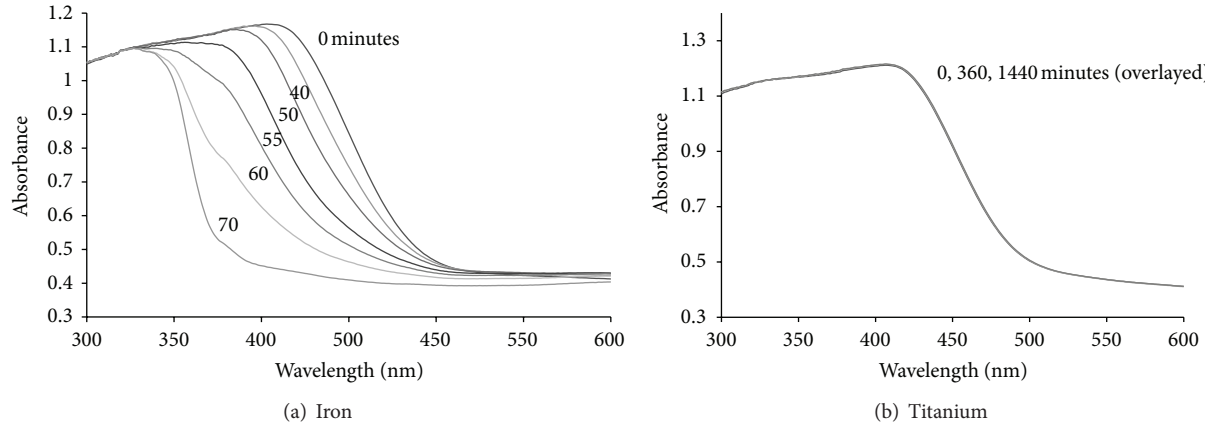

(a) Iron (b) Titanium

Figure 3: DR UV/Vis absorbance spectra of I_3^- and corrosion rate recorded in reflectance setup for encapsulation cells using (a) iron and (b) titanium.

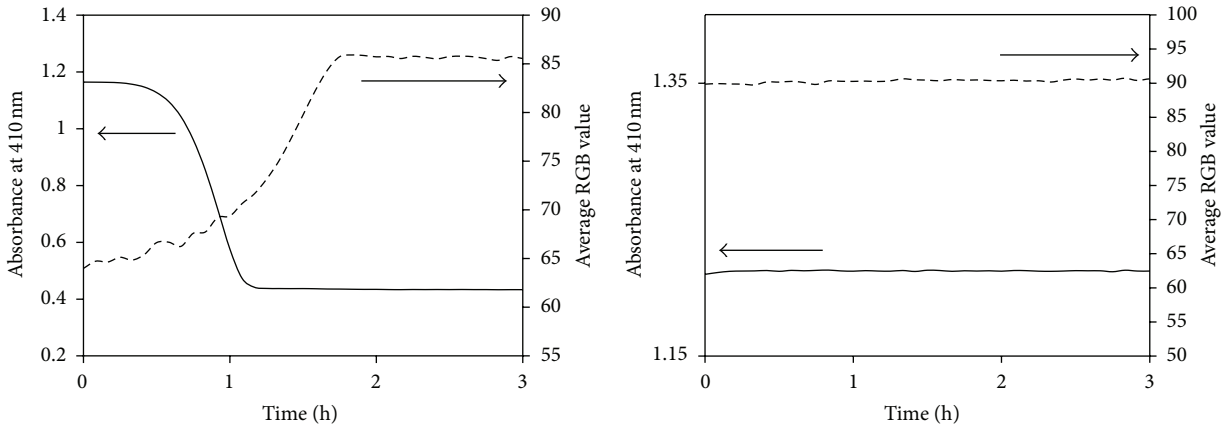

(a) Iron (b) Titanium

Figure 4: Changes of electrolyte composition according to time-dependant decrease in DR-UV/Vis absorption at 410 nm and average colour intensity (RGB) as measured using time-lapse photography for (a) iron and (b) titanium.

hours for both analytical methods. For the encapsulation cell experiments carried out here, it was observed that a rapid decrease in the I_3^- concentration was observed immediately and continued over the ensuing 2-hour period. A complete and irreversible disappearance of the I_3^- occurred as shown in Figure 4. The subtle variation in the apparent corrosion times between the two methods reflects the slight changes in electrolyte volume within each encapsulated cell. This is quite difficult to control accurately since the seal is made using a heated Surlyn gasket which, although nominally 25 μm, is subject to compression. The corrosion of iron seen in this work is not consistent with previous observations of carbon steel corrosion. However, these authors immersed the steel in significantly larger volumes of DSC electrolyte than the estimated 0.015 cm^3 quantity introduced to the encapsulation cells employed here. This result illustrates the importance of studying the corrosion in assembled model cells rather than in immersion conditions. In our system, there was no visible iron corrosion at the point of complete electrolyte discolouration. The result raises significant doubts about the suitability of carbon steel as a potential DSC substrate because the stability in the presence of I_3^- is temporary.

The tests carried out in Figures 3 and 4 have used a simple three-component electrolyte. Typically other components are added to enhance the photovoltaic performance of the device such as nitrogen containing heterocyclics. The most popular electrolyte addition is tert-butylpyridine (TBP) which adsorbs onto bare TiO_2 and suppresses back electron transfer to the electrolyte from the TiO_2 conduction band [21]. TBP is used most frequently at 0.5 M concentration. Figure 5 shows the result of electrolyte colour change with and without TBP recorded using the photographic method.

As mentioned previously, the disappearance of the triiodide is complete within 2 hours using an electrolyte that does not contain TBP; however, when it is included (at 0.5 M) in the electrolyte, no corrosion is observed, even for periods of many months. This is a critical finding in the measuring of corrosion phenomenon in contact with dye-sensitized solar cell electrolytes and can go some way to explain the discrepancies in the literature on performance

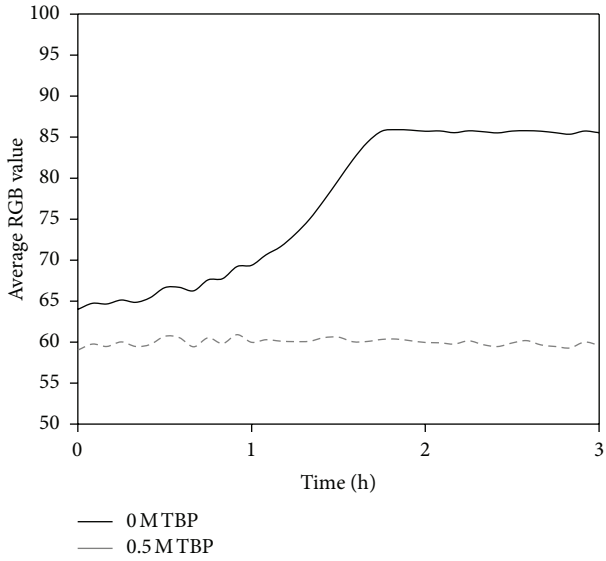

Figure 5: Changes of electrolyte determined using average red green and blue (RGB) values for a triiodide electrolyte with and without 0.5 M TBP. The electrolyte contained 0.1 M LiI and 0.05 I_2 in methoxypropionitrile.

[2, 22]. Often nitrogen containing heterocyclics are used in different forms (tert-butylpyridine, benzimidazole, etc.) without consideration to their effect on the corrosion of the substrate. Clearly, the TBP acts as a corrosion inhibitor on the surface of the iron, improving its corrosion resistance in the presence of the I_3^-/I^- electrolyte. For clarity and to elucidate the corrosiveness of the iodide/triiodide couple, the TBP has been left out of the electrolyte for the rest of the programme described here. Further experimentation is underway to determine if additive corrosion inhibition can affect stability of electrolytes and this will be reported separately.

Encapsulated model DSC corrosion cells prepared on titanium substrates showed an exceptionally stable outcome over the time period of the experiment; this is clearly shown in Figure 4(b). No change in average intensity or triiodide absorbance data was observed over the experiment timeframe and is consistent between both techniques. This is an entirely expected result as titanium is presently considered to be the substrate of choice for metal-based dye-sensitized solar cells [3, 5, 8].

The obvious expense associated with titanium for large scale manufacture is driving the search for alternative substrate materials. A range of metals was then tested to identify stable materials using the simple RGB method described previously. The performance of these materials is presented in Table 2 and discussed separately with an initial focus on architectural substrates such as zinc and aluminium.

Table 2 illustrates that many of the structural metals could be used either in their own right or as alloying elements or metallic coatings for iron which may suffer from corrosion (in the absence of corrosion inhibiting species such as TBP). This data is also important in illustrating once more the value of the photographic method. Although rapid corrosion kinetics can be recorded with the DR-UV/Vis method, obviously the photographic method is more convenient for items that resist corrosion for longer.

Table 2: Summary of corrosion performance for a range of metal substrates determined using time-lapse photographic analysis (up to 1000 hrs).

Metal type (0.05 M I_2 + 0.5 M LiI in MPN)	Time to complete I_3^- removal (h)
Titanium	—
Iron 99.5%	2
Stainless steel (316 and 304)	—
Zinc 99.9%	0.03
Aluminium 99.0%	—
Aluminium 99.0% surface activation	30
Aluminium 99.999% surface activation	~200
Nickel 99.98%	~65
Inconel (625)	—
Tungsten 99.95%	—
Molybdenum 99.9%	—
Chromium 99.95%	—

3.1. Zinc and Aluminium. Zinc and aluminium are used as metallic coatings for iron in commercial structural metals applications. Of the metals in the various encapsulation cells prepared in this study zinc (Zn) substrates by far show the most rapid reaction with the electrolyte solution. At the instant the I_3^- containing electrolyte was introduced to the Zn encapsulation cells a visible loss of colour was detected. Within 2 min, the electrolyte layer had become colourless, signifying the complete reduction of I_3^- to I^- according to reaction (2) and the subsequent oxidation of metallic zinc to release Zn^{2+} ions. The overall reaction is represented by (3) as follows.

$$Zn + I_3^- \longrightarrow Zn^{2+} + 3I^-. \quad (3)$$

The poor corrosion resistance of Zn observed here confirms the findings of Toivola et al. [2] using a method based on the immersion of metal coupons in millilitre quantities of DSC electrolyte. Although these authors state that the reaction takes place over a series of days, their findings are not inconsistent with the speed of reaction observed in this present study as the absolute quantity of I_3^- used here in the encapsulation cells will be several orders of magnitude less and will consequently be completely consumed more rapidly. The findings therefore suggest that any metal strip product incorporating a galvanizing technology as corrosion protection would also be wholly unsuitable as a potential substrate for direct fabrication of DSCs. Further work is in progress to evaluate how corrosion inhibiting species in the electrolyte are able to stabilise the corrosion reactions.

The corrosion of aluminium in the presence of the electrolyte has been reported by others [6]. In our investigation,

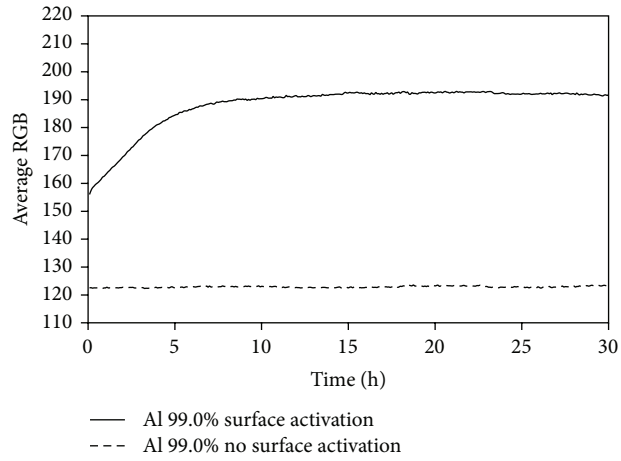

Figure 6: Changes of electrolyte determined using average red, green, and blue (RGB) values for a tri-iodide electrolyte on an aluminium substrate with different surface activations.

preliminary experiments carried out on as-received aluminium substrates of varying purity showed, perhaps surprisingly, that rates of tri-iodide disappearance were negligible over a timescale of many days. However, further experiments using the same substrates following abrasive cleaning gave contradictory findings, where complete removal of tri-iodide was observed over the same durations. Therefore, key to the initiation of corrosion on Al is the nature of surface treatment. The as-received substrate will comprise an air-formed surface oxide layer which as these tests demonstrate possesses sufficiently effective barrier properties to protect the underlying metal from oxidation via reaction (2). Surface abrasion not only removes this original protective layer, but is also well known to introduce a surface activated layer, with significantly different corrosion behaviour to the bulk [23]. This phenomenon has been reported on 3000, 5000, 6000 and 8000 series aluminium alloys and can lead to rapid chloride-induced filiform-like corrosion on organic coated substrates [24–29]. It has been proposed that micrograining of the surface layer, induced by abrasion, produces a significant anodic activation compared with the alloy bulk [30, 31]. In this work, it can be seen that the aluminium samples even with relatively low purity can resist corrosion, providing that they are not subjected to initial surface abrasion. Figure 6 shows the difference between as-received and abraded Al specimens of 99.9% purity, where the abraded sample has reacted to completely remove triiodide from the electrolyte layer within 20 hours, whilst the nonabraded Al remains stable.

It is also evident from Table 2 that the rate of reaction obtained for abraded Al specimens is highly dependent upon purity. The observed rate of disappearance of tri-iodide is approximately 7-fold higher in the presence of a low purity (99.0%) specimen than observed for higher purity (99.999%) Al. It is proposed that the increase in rate results from the greater availability of transition metal impurity phases, which in turn will provide a greater number of sites of high electrocatalytic activity for the reduction of tri-iodide.

3.2. Nickel, Chromium, and Nickel-Chromium Alloys. Pure nickel, chromium, and Inconel 625, a nickel chromium alloy were also investigated as potential substrates. It is clear from this data that Ni exposed in our system corrodes. It should be noted that Ma et al. [6] found nickel to be stable in an I_3^-/I^- electrolyte solution. Here, again, we have used very small electrolyte volumes in the cells and so there is extremely high sensitivity to even small amounts of corrosion. It is also the case that with these authors a more fully formulated electrolyte was used and this further raises the intriguing possibility that nonelectron mediating components of the electrolyte may be playing a role in substrate corrosion inhibition. The alloy Inconel 625's performance over the 1000 hours time period seems to be stable regarding corrosion and this is consistent given the demonstrated manufacture of cells on this substrate [12, 32].

3.3. Molybdenum, Tungsten, and Stainless Steel. The final group of potential metal substrates tested was better known for their corrosion resistance when exposed to more aggressive environments. Stainless steel, molybdenum, and tungsten showed stability with a DSC electrolyte environment even in the absence of any corrosion inhibiting additives. Encapsulation cells prepared on these substrates showed an exceptionally stable outcome over the time period of the experiment. No change in average intensity or tri-iodide absorbance data was observed over the experiment timeframe.

4. Conclusion

The two methods reported here for monitoring the colour of the electrolyte exposed in a confined environment based on tri-iodide provide complimentary insights into the corrosion of metal substrates for dye-sensitized solar cells. It is important to use manufactured model cells since these reflect the real corrosion atmosphere upon exposure. The very small quantities of electrolyte also highlight corrosion issues prior to any observable corrosion on the metal surfaces. Key findings of this initial study are that titanium, tungsten, molybdenum, chromium, Inconel, and stainless steel demonstrate stability in the presence of a simple DSC electrolyte formulation. These materials can therefore be considered as potential substrates for DSC manufacture. The issue then is cost.

Iron, however, is not resistant to corrosion, whereby carbon steel has been reported as stable in some literature. In the case of iron, this is likely to result from the corrosion inhibiting effects that certain electrolyte additions have, which we have also demonstrated. Further work is in progress to evaluate how nitrogen containing heterocyclics can influence the corrosion reactions on iron and other metals since they may offer a lifetime extension and expand the range of stable metals that can be used.

Aluminium (99.9%) does not corrode over many months exposure in a model cell. However, surface preparation by abrasion activates the surface and even aluminium with higher purity (99.999%) will corrode at this point. Again,

this is important information since in any manufacturing environment it is likely that surface damage could occur and activate the material. Overall, the photographic method with image analysis is perhaps the most convenient of the two techniques since it is cheaper and allows for simultaneous multi-sample analysis.

Conflict of Interests

The authors do not have any conflict of interests with the content of the paper.

Acknowledgments

The authors would like to thank the EPSRC and TSB for supporting this work through the SPECIFIC Innovation and Knowledge Centre. The authors would also like to gratefully acknowledge the Welsh Government and ERDF Low Carbon Research Institute (LCRI) convergence funding through the Solar Photovoltaic Academic Research Consortium (SPARC-Cymru). In addition, The authors would like to acknowledge the funding by the European Social Fund (ESF) through the European Union's Convergence programme administered by the Welsh Government.

References

[1] B. O'Regan and M. Grätzel, "A low-cost, high-efficiency solar cell based on dye-sensitized colloidal TiO_2 films," *Nature*, vol. 353, pp. 737–740, 1991.

[2] M. Toivola, F. Ahlskog, and P. Lund, "Industrial sheet metals for nanocrystalline dye-sensitized solar cell structures," *Solar Energy Materials and Solar Cells*, vol. 90, no. 17, pp. 2881–2893, 2006.

[3] T. M. Watson, G. J. Reynolds, and D. A. Worsley, "Painted steel mounted dye sensitised solar cells: titanium metallisation using magnetron sputtering," *Ironmaking and Steelmaking*, vol. 38, no. 3, pp. 168–172, 2011.

[4] X. Fang, T. Ma, M. Akiyama, G. Guan, S. Tsunematsu, and E. Abe, "Flexible counter electrodes based on metal sheet and polymer film for dye-sensitized solar cells," *Thin Solid Films*, vol. 472, no. 1-2, pp. 242–245, 2005.

[5] S. Ito, N. L. C. Ha, G. Rothenberger et al., "High-efficiency (7.2%) flexible dye-sensitized solar cells with Ti-metal substrate for nanocrystalline-TiO_2 photoanode," *Chemical Communications*, vol. 38, pp. 4004–4006, 2006.

[6] T. Ma, X. Fang, M. Akiyama, K. Inoue, H. Noma, and E. Abe J, "Properties of several types of novel counter electrodes for dye-sensitized solar cells," *Journal of Electroanalytical Chemistry*, vol. 574, no. 1, pp. 77–83, 2004.

[7] K. Onoda, S. Ngamsinlapasathian, T. Fujieda, and S. Yoshikawa, "The superiority of Ti plate as the substrate of dye-sensitized solar cells," *Solar Energy Materials and Solar Cells*, vol. 91, no. 13, pp. 1176–1181, 2007.

[8] K. Kalyanasundaram, S. Ito, S. Yanagida, and S. Uchida, "Scale up and product development studies of dye-sensitized solar cells in Asia and Europe," in *Dye-Sensitized Solar Cells*, K. Kalyanasundaram, Ed., chapter 9, pp. 267–321, EPFL Press, Lausanne, Switzerland, 2010.

[9] Y. Jun, J. Kim, and M. G. Kang, "A study of stainless steel-based dye-sensitized solar cells and modules," *Solar Energy Materials and Solar Cells*, vol. 91, no. 9, pp. 779–784, 2007.

[10] T. Watson, I. Mabbett, H. Wang, L. Peter, and D. Worsley, "Ultrafast near infrared sintering of TiO_2 layers on metal substrates for dye-sensitized solar cells," *Progress in Photovoltaics: Research and Applications*, vol. 19, no. 4, pp. 482–486, 2011.

[11] T. Tsai, C. Chen, S. Cherng, and S. Suen, "An efficient titanium-based photoanode for dye-sensitized solar cell under back-side illumination," *Progress in Photovoltaics*, vol. 21, pp. 226–231, 2013.

[12] K. Miettunen, X. Ruan, T. Saukkonen et al., "Stability of dye solar cells with photoelectrode on metal substrates," *Journal of the Electrochemical Society*, vol. 157, no. 6, pp. B814–B819, 2010.

[13] K. Miettunen, J. Halme, and P. Lund, "Segmented cell design for improved factoring of aging effects in dye solar cells," *Journal of Physical Chemistry C*, vol. 113, no. 23, pp. 10297–10302, 2009.

[14] K. Miettunen, J. Halme, M. Toivola, and P. Lund, "Initial performance of dye solar cells on stainless steel substrates," *Journal of Physical Chemistry C*, vol. 112, no. 10, pp. 4011–4017, 2008.

[15] T. Watson, P. Holliman, and D. Worsley, "Rapid, continuous in situ monitoring of dye sensitisation in dye-sensitized solar cells," *Journal of Materials Chemistry*, vol. 21, no. 12, pp. 4321–4325, 2011.

[16] M. I. Asghar, K. Miettunen, S. Mastroianni, J. Halme, H. Vahlman, and P. Lund, "In situ image processing method to investigate performance and stability of dye solar cells," *Solar Energy*, vol. 86, no. 1, pp. 331–338, 2012.

[17] M. Carnie, D. Bryant, T. Watson, and D. Worsley, "Photocatalytic oxidation of triiodide in UVA-exposed dye-sensitized solar cells," *International Journal of Photoenergy*, vol. 2012, Article ID 524590, 2012.

[18] T. Watson, C. Charbonneau, D. Bryant, and D. Worsley, "Acid treatment of titania pastes to create scattering layers in dye-sensitized solar cells," *International Journal of Photoenergy*, vol. 2012, Article ID 637839, 8 pages, 2012.

[19] H. Kusama and H. Arakawa, "Influence of benzimidazole additives in electrolytic solution on dye-sensitized solar cell performance," *Journal of Photochemistry and Photobiology A: Chemistry*, vol. 162, no. 2-3, pp. 441–448, 2004.

[20] Z. Yu, M. Gorlov, G. Boschloo, and L. Kloo, "Synergistic effect of N-methylbenzimidazole and guanidinium thiocyanate on the performance of dye-sensitized solar cells based on ionic liquid electrolytes," *Journal of Physical Chemistry C*, vol. 114, no. 50, pp. 22330–22337, 2010.

[21] M. K. Nazeeruddin, A. Kay, R. Humpbry-baker et al., "Conversion of light to electricity by cis-X2bis(2,2'-bipyridyl-4,4'-dicarboxylate)ruthenium(II) charge-transfer sensitizers (X = Cl-, Br-, I-, CN-, and SCN-) on nanocrystalline titanium dioxide electrodes," *Journal of the American Chemical Society*, vol. 115, no. 14, pp. 6382–6390, 1993.

[22] K. Miettunen, J. Halme, and P. Lund, "Metallic and plastic dye solar cells," *Wiley Interdisciplinary Reviews: Energy and Environment*, vol. 2, no. 1, pp. 104–120, 2013.

[23] H. N. McMurray and G. Williams, "Under film/coating corrosion," in *Shreir's Corrosion*, T. A. J. Richardson, Ed., chapter 2.14, pp. 988–1004, Elsevier, 4th edition, 2009.

[24] H. Leth-Olsen, A. Afseth, and K. Nisancioglu, "Filiform corrosion of aluminium sheet. II. Electrochemical and corrosion behaviour of bare substrates," *Corrosion Science*, vol. 40, no. 7, pp. 1195–1214, 1998.

[25] H. Leth-Olsen, J. H. Nordlien, and K. Nisancioglu, "Filiform corrosion of aluminium sheet. III. Microstructure of reactive surfaces," *Corrosion Science*, vol. 40, no. 12, pp. 2051–2063, 1998.

[26] H. Leth-Olsen and K. Nisancioglu, "Filiform corrosion of aluminium sheet. I. Corrosion behaviour of painted material," *Corrosion Science*, vol. 40, no. 7, pp. 1179–1194, 1998.

[27] X. Zhou, G. E. Thompson, and G. M. Scamans, "The influence of surface treatment on filiform corrosion resistance of painted aluminium alloy sheet," *Corrosion Science*, vol. 45, no. 8, pp. 1767–1777, 2003.

[28] Y. Liu, X. Zhou, G. E. Thompson, T. Hashimoto, G. M. Scamans, and A. Afseth, "Precipitation in an AA6111 aluminium alloy and cosmetic corrosion," *Acta Materialia*, vol. 55, no. 1, pp. 353–360, 2007.

[29] R. Ambat, A. J. Davenport, A. Afseth, and G. Scamans, "Electrochemical behavior of the active surface layer on rolled aluminum alloy sheet," *Journal of the Electrochemical Society*, vol. 151, no. 2, pp. B53–B58, 2004.

[30] H. N. McMurray, A. J. Coleman, G. Williams, A. Afseth, and G. M. Scamans, "Scanning kelvin probe studies of filiform corrosion on automotive aluminum alloy AA6016," *Journal of the Electrochemical Society*, vol. 154, no. 7, pp. C339–C348, 2007.

[31] H. N. McMurray, A. Holder, G. Williams, G. M. Scamans, and A. J. Coleman, "The kinetics and mechanisms of filiform corrosion on aluminium alloy AA6111," *Electrochimica Acta*, vol. 55, no. 27, pp. 7843–7852, 2010.

[32] G. Hashmi, K. Miettunen, T. Peltola et al., "Review of materials and manufacturing options for large area flexible dye solar cells," *Renewable and Sustainable Energy Reviews*, vol. 15, no. 8, pp. 3717–3732, 2011.

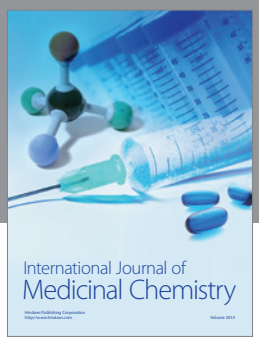

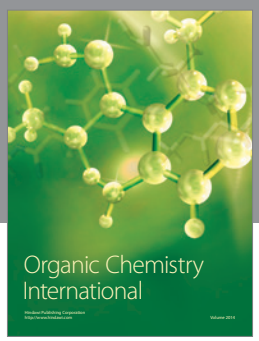

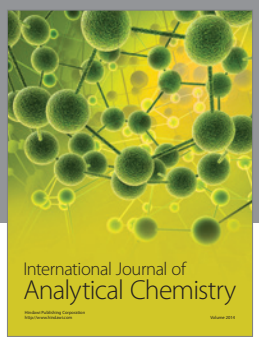

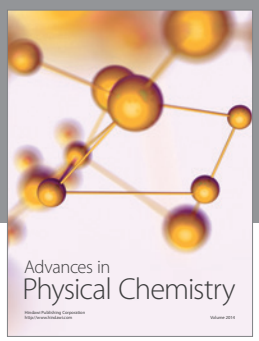

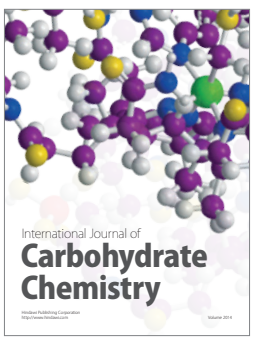

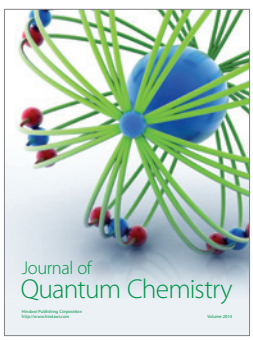

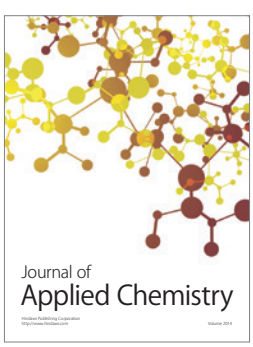

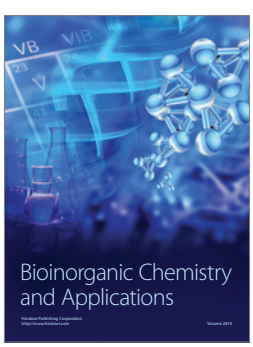

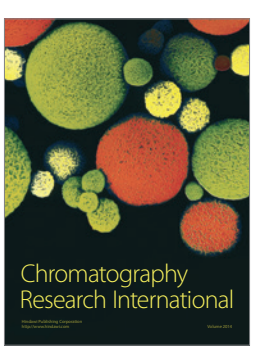

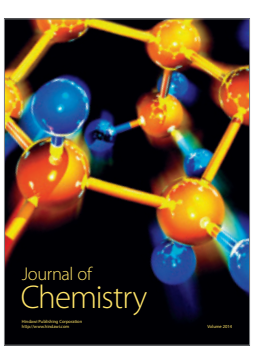

Hindawi

Submit your manuscripts at
http://www.hindawi.com